engineering proceedings

MDPI

Proceeding Paper

Induction Motor Energy Efficiency Investigation †

István Szénásy * and Dániel Csikor

Vehicle Industry Research Center, Széchenyi István University, 9026 Győr, Hungary; csikor.daniel@ga.sze.hu
* Correspondence: szenasy@sze.hu
† Presented at the Sustainable Mobility and Transportation Symposium 2024, Győr, Hungary, 14–16 October 2024.

Abstract: The energy efficiency of the induction motor (IM) is extremely important in the drives of electric vehicles. The first part of the article examines the possibilities of modifying the torque and efficiency curves in order to realize high-torque work points more efficiently by modifying the motor's impedances. Later, it analyzes the flux-dependent changes in the highly load-dependent efficiency based on the literature. The FEM-type investigations of the experimental IM development carried out at the Vehicle Industry Research Center Institute of the Széchenyi István University offer new control options for increasing the efficiency of work points with lower torque and speed as well as for modifying the examined torque curve sections.

Keywords: deep bars rotor IM induction motor; flux-dependent losses; IM online efficiency control

1. Introduction

The high efficiency of the IM is extremely important for electric vehicles being driven using batteries. Its effectiveness is highly load-dependent. In vehicle drives, torque around the nominal is needed for a short time, so the motor mostly operates at a partial load with a lower efficiency. This disadvantage can be improved with control devices, and the magnetic flux can be reduced to an optimal level. Another theme is the approximation of the torque-efficiency curves to a higher efficiency at high-torque points by modifying the impedances of the rotor. At the Széchenyi István University, a 100 kW/700 Nm/380 V power induction motor suitable for vehicle propulsion was developed and analyzed using FEM-type Infolytica software.

Energy-optimal operation is an essential aspect when planning drives. Losses increase energy demand and generate heat, which must be dissipated by additional measures and constructive efforts. Modern power electronic devices achieve an efficiency of over 98%, and medium- and high-performance IM motors achieve an efficiency of over 92–95% at the nominal operating point. At a partial load, however, the efficiency can decrease significantly. The reason is that the absorbed magnetizing current does not depend on the load, but on the terminal voltage of the motor. In operation at a lower torque, the flux can be lower, and the losses depend on the current and the flux. Worldwide model-based and hybrid research methods minimize the loss performance by adapting the flux online. The shown method selects the conditions for the best efficiency by examining the motor model, and the vehicle control helps this too.

2. Materials and Methodology

It is a well-known characteristic of IMs that the maximum locations of the torque–slip and the efficiency–slip curves do not coincide, so the upper points of the torque curves can be used only with a reduced efficiency. The reduction can be up to 20%, depending on the geometry of the rotor cage. This cannot be influenced by control methods. Figure 1 shows the characteristic curves of a standard IM with a cage; the maximum values of the efficiency (green) and torque (red) curves here are shifted from each other.

check for updates

Citation: Szénásy, I.; Csikor, D. Induction Motor Energy Efficiency Investigation. *Eng. Proc.* **2024**, *79*, 75. https://doi.org/10.3390/engproc2024079075

Academic Editors: András LajosNagy, Boglárka Eisinger Balassa, László Lendvai and Szabolcs Kocsis-Szürke

Published: 11 November 2024

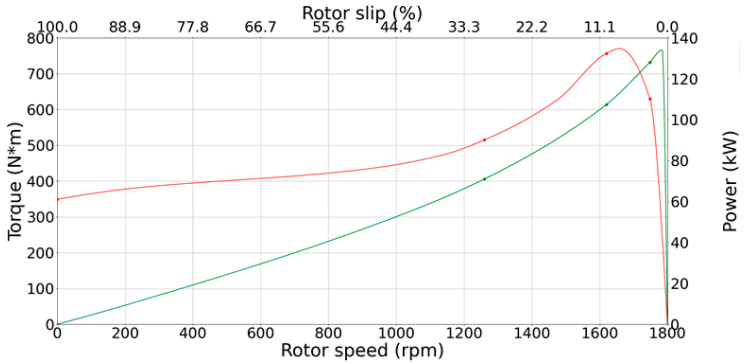

Figure 1. Mutual positions of torque and efficiency curves in IM.

Deep-slot rotors using the principle of current displacement have been known and used mainly to increase the starting torque [1–4]. This principle is based on the skin effect, which results in a higher current density in the induction motor near the air gap in the cross-section of the rotor bars. An increase in the resistance, together with a decrease in the leakage inductance, results in a lower starting current and a higher starting torque. Changes in the values of the resistance and inductance can also be calculated analytically [5]. In the case of a rectangular bar shape, with a groove depth h and stray inductance σ, it can be calculated with the following expressions [3], where the coefficients k_r and k_x are functions of h/σ.

$$k_r = \frac{r}{r_0} = \frac{R'_2}{R'_{20}} = \frac{h}{\sigma}\frac{sh\left(\frac{2h}{\sigma}\right) + \sin\left(\frac{2h}{\sigma}\right)}{ch\left(\frac{2h}{\sigma}\right) - \cos\left(\frac{2h}{\sigma}\right)} \quad (1)$$

$$k_x = \frac{L}{L_0} = \frac{L'_2}{L'_{20}} = \frac{3\sigma}{2h}\frac{sh\left(\frac{2h}{\sigma}\right) - \sin\left(\frac{2h}{\sigma}\right)}{ch\left(\frac{2h}{\sigma}\right) - \cos\left(\frac{2h}{\sigma}\right)} \quad (2)$$

This is proportional to $\sqrt{s}$, so kr and kx are also functions of slip; see Figure 2a (rotor frequency).

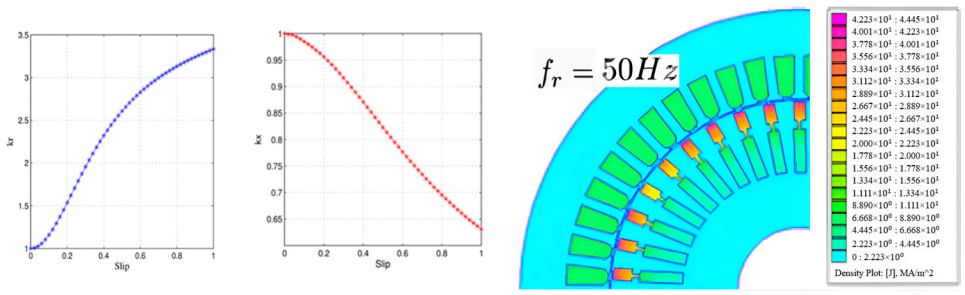

(**a**) (**b**) (**c**)

Figure 2. The frequency dependence of the coefficient for the analytical calculation of the current density (**a**,**b**); the current density at a given slip-frequency (**c**).

The disadvantage of the analytical method is that it can be used for uniform geometries only. Various improvements in the solution have appeared, expanding the possibilities for more complicated geometries [5,6].

Numerical methods use FEM software to calculate the rotor impedance. Figure 2a,b present the frequency dependence of the coefficient for the analytical calculation of the current density [3,7]. Figure 2c shows the current density at a given slip-frequency. The values at 50 Hz are about 2 A/mm^2 in the inner bars and 40 A/mm^2 in the outer bars.

A steady-state, analytical IM modeling is presented that represents the behavior of these IMs during operation. Figure 3a shows an equivalent scheme with variable rotor parameters [2,7].

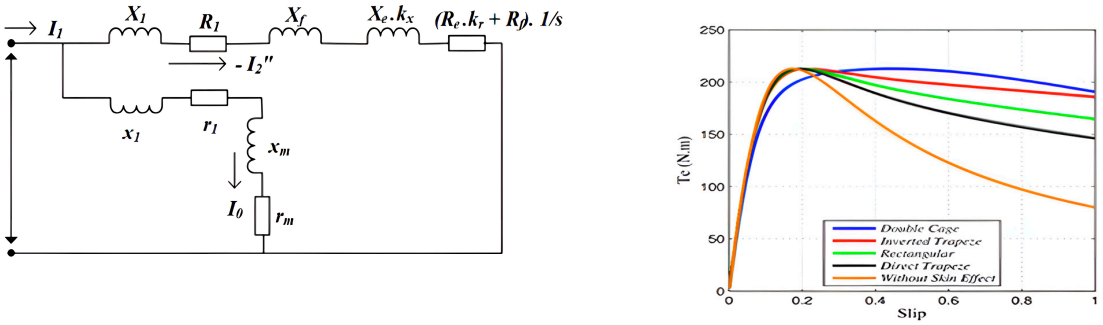

(**a**) (**b**)

Figure 3. Equivalent schemes of a deep bar with rotor parameters (**a**), torque curves by I_2'' (**b**).

R_e and X_e are the resistance of the rotor and leakage reactance of the bar calculated for the stator, respectively; R_f and X_f are the resistance and reactance of the rotor of the front part calculated back to the stator, respectively. Figure 3b shows torque curves as a function of the slip for different cage designs. Based on Figure 3b, the torque can be expressed as follows.

$$T_e = \frac{m_1 V_1^2 \left(\frac{k_r R_e + R_f}{s}\right)}{\Omega_1 \left[\left(R_1 + \left(\frac{k_r R_e + R_f}{s}\right)\right)^2 + \left(X_1 + \left(k_x X_e + X_f\right)\right)^2\right]} \quad (3)$$

A steady-state, analytical IM modeling represents the behavior of these IMs during operation [3].

By adjusting the impedances of the cage rotor, the torque curve can be shifted to the right, so that the maximum torque and maximum efficiency operating points are closer together. In the absence of research results, it was necessary to use FEM software, and with this, it was possible to examine the characteristics of many single- and double-cage motors with different geometries. With the available impedance changes, the result was a two-cage linkage, which shifts the upper section of the torque–slip curve to the right, realizing the possibility of higher efficiency and high-torque operation. Figure 4 shows results that are realized with the rotor in Figure 4a made of Cu (or Al) material bars at an intersection with a better efficiency value on the efficiency curve [8–11].

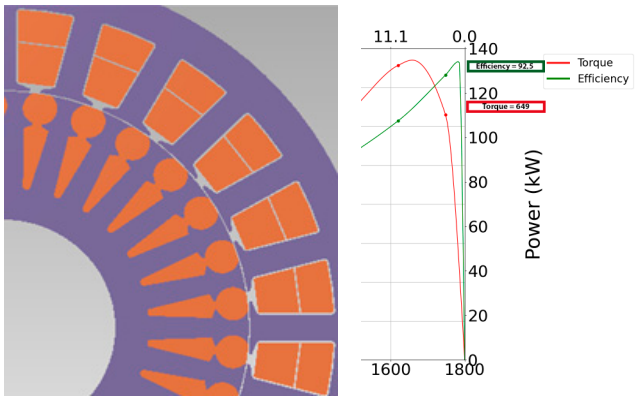

(**a**) (**b**)

Figure 4. The form of the double-cage rotor with the best result (**a**); its effects at 120 kW power, 92.5% efficiency, and 0.759 cos φ (**b**).

3. FEM-Type Research and Development

IMs open up new research and planning opportunities. In the process of planning and measuring, the IM simulations enable preliminary knowledge of the motor and discovery

of its properties and parameters. With FEM-type Infolytica software has been developed a 4 p/100 kW/700 Nm/380 V/60 Hz power IM induction motor suitable for a vehicle drive that is suitable for principle examination and construction. This is also how the detailed diagrams were prepared, which enable the presentation of the changes caused in the motor's load conditions and their consequences. The effects of the voltage reduction on the increase in efficiency and loss ratios are visible changes. In addition to the terminal voltage and frequency parameters, the output power and torque, the current, the slip, the efficiency, the cos φ, and the changes in the loss power can be seen as functions of the rotor speed.

At f = 60Hz, T = 51.6 Nm, P_{out} = 9.62 kW, U = 136 V_{rms} only, s = 1.03 %, the efficiency is 95.3 %, so reduced performance does not impair efficiency. In Figure 5, at an extremely low speed of 18 rpm, the torque is 480 Nm and the efficiency is 7.63%. In this case, the excitation is 1.2 Hz.

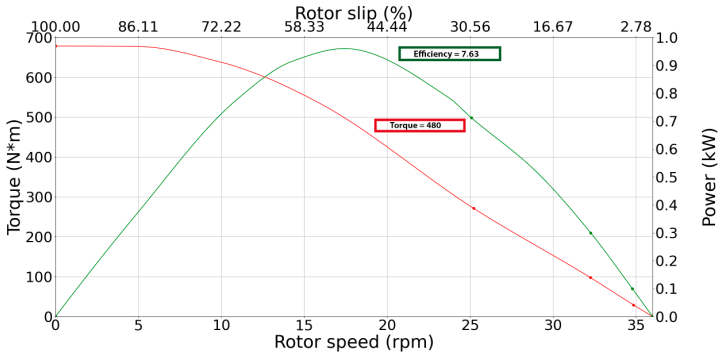

Figure 5. Extreme low speed: frequency 2% = 1.2 Hz, n_0 = 36 rpm, 24 V_{rms}, 480 Nm, s 50%, n 18 rpm = 3.33 s/one turn, eff. = 7.63%, loss total = 11 kW, U = 7.6 V_{rms}.

4. Results

We carried out controlled drive tests with the electric motor model. The results of the performed runs can be seen at the Al cage IM in Figure 6. The orange cross + indicates the torque from the pedal position. Blue numerical values are the voltages required to achieve the best efficiency for each working point. Shown in green are the efficiency values realized during the runs, and in black are the values of the slip required for the specified torque, keeping the regulation at a given value. To maintain a given torque level, the motor receives the voltage corresponding to the current speed, the given value of the slip provides the desired torque, and the speed increases the voltage as V/f. This can be seen at voltages of the same torque at increasing speeds in Figure 6. It can be stated that for the high-efficiency control of a newly developed IM, it is advisable to use design software that calculates the voltage demand of a given torque and the performance, the losses, and the efficiency for any speed during the simulations.

By changing the slip, the best efficiency for the given torque and speed can be obtained, which is intended to be realized in actual operation.

In the management of the vehicle control, the voltage is set by the control system, according to the actual torque signal and speed, by a LUT or by other predefined functions. A possible solution is a polynomial created by curve fitting that calculates the actual voltage as a function of the speed and the torque demand, T:

$$U = ax^3 + bx^2 + cx + d_1 + T * d_2 \quad (4)$$

The values d_1 and d_2 can also depend on the rate of change in the torque set-point dT/dt, improving the dynamic properties of the drive with sign pre-correction. Considering that vehicle drives are systems with greater inertia, changing the dynamic state is a slower process, so more time is available for control interventions. It is also possible to estimate the

process of future work points based on the nature of the torque level increase. The needed slip s can also be written as a function of speed x and torque T:

$$s = 100 - a_1 x^2 - b_1 x + T * d_3, \ [\%] \tag{5}$$

The coefficients a_1, b_1, and d_3 are determined by taking into account the characteristics of the drive system.

The driver's intention regarding motor torque is indicated by the pedal position. The required motor voltage at the current speed is based on knowledge of the motor's data fields and is calculated as a function of the speed, e.g., every 10 ms, and changes the voltage with the inverter, with a relatively large time constant. The actual change in torque brings an inherent change in the slip, which is modified by the small change in the frequency of the inverter as slip control, with a small time constant. The actual slip value is recalculated every few ms from the rotor speed and the current frequency.

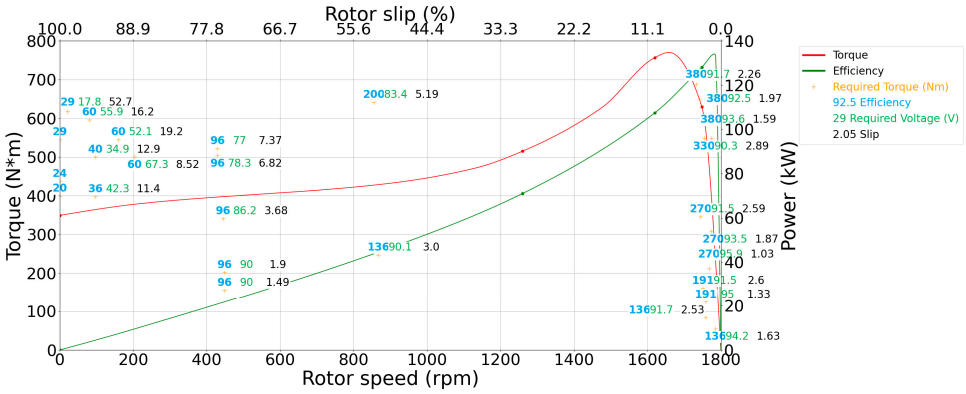

Figure 6. The summary results of the performed runs.

5. Summary and Conclusions

With the help of FEM software, we have examined the properties of cage-induction motors with different geometries. With the changes in impedance that can be achieved by modifying the bar geometry, the best result was obtained with a double-cage bar system, which shifted the upper section of the torque–slip curve to the right, realizing the possibility of higher efficiency and high-torque operation. A control feature is that the required motor voltage is calculated as a function of the speed based on the knowledge of the motor's data fields, and it ensures the realization of the pre-planned torque and efficiency. When the real IM-driven vehicle is running, the actual working points realize the predetermined best-efficiency torque levels. Another result of the implemented bar geometry research was a high, even starting torque. With FEM design software, it was possible to plan and examine in detail the properties of the 100 kW IM and the loss analyses. All these made it possible to develop a new management strategy for IMs.

Author Contributions: Conceptualization, I.S.; methodology, I.S.; software, D.C.; validation, I.S.; formal analysis, I.S.; investigation, I.S.; resources, D.C.; data curation, I.S.; writing—original draft preparation, I.S.; writing—review and editing, D.C.; visualization, I.S.; supervision, I.S.; project administration, D.C.; funding acquisition, I.S. All authors have read and agreed to the published version of the manuscript.

Funding: The research was supported by the European Union within the framework of the National Laboratory for Autonomous Systems (RRF-2.3.1-21-2022-00002).

Institutional Review Board Statement: Not applicable.

Informed Consent Statement: Not applicable.

Data Availability Statement: The raw data supporting the conclusions of this article will be made available by the authors on request.

Conflicts of Interest: The authors declare no conflict of interest.

References

1. Williamson, S.; Gersh, D.R. Finite element calculation of double-cage rotor equivalent circuit parameters. *IEEE Trans. Energy Convers.* **1996**, *11*, 41–48. [CrossRef]
2. Benecke, M.; Doebbelin, R.; Griepentrog, G.; Lindemann, A. Skin effect in squirrel cage rotor bars in simulation of non-steady-state operation of induction machines. *PIERS* **2010**, *7*, 421–425.
3. Maddi, Z.; Aouzellag, D. Dynamic Modelling of Induction Motor Squirrel Cage for Different Shapes of Rotor Deep Bars with Estimation of the Skin Effect. *Prog. Electromagn. Res.* **2017**, *59*, 147–160. [CrossRef]
4. Maddi, Z.; Abdoune, K. Skin Effect Modelling in Induction Motors Rotor Deep Bars. In Proceedings of the International Conference on Electronics and Electrical Engineering, Bouira, Algeria, 12–13 November 2018.
5. Gheorghe, C.M.; Melcescu, L.M.; Tudorache, T.; Mihai, E. Numerical modeling approaches for the analysis of squirrel-cage induction motor. *Rev. Roum. Sci. Techn.–Électrotechn. Énerg.* **2016**, *61*, 18–21.
6. Szenasy, I. Magnet Losses of Fractional Number Slots Per Pole PMSM in Flux Weakening Operation. In Proceedings of the 2013 IEEE 10th International Conference on Power Electronics and Drive Systems (PEDS), Kitakyushu, Japan, 22–25 April 2013. [CrossRef]
7. Boglietti, A.; Cavagnino, A.; Lazzari, M. Computational algorithms for induction-motor equivalent circuit parameter determination—Part I: Resistances and leakage reactances. *IEEE Trans. Ind. Electron.* **2010**, *58*, 3723–3733. [CrossRef]
8. Uddin, M.N.; Nam, S.W. New online loss-minimization-based control of an induction motor drive. *IEEE Trans. Power Electron.* **2008**, *23*, 926–933. [CrossRef]
9. Nguyen, P.; Quang, J.D. *Vector Control of Three-Phase AC Machines*; Springer: Heidelberg, Germany, 2008.
10. Szenasy, I.; Varga, Z. Features of segment winded PMSM for a low voltage supply system. In Proceedings of the 2017 3rd International Conference on Control, Automation and Robotics (ICCAR), Nagoya, Japan, 24–26 April 2017. [CrossRef]
11. Szenasy, I.; Varga, Z.; Szeli, Z. Optimum control strategy for PMSM in field-weakening region by constant power. In Proceedings of the 2015 International Conference on Electrical Systems for Aircraft, Railway, Ship Propulsion and Road Vehicles (ESARS), Aachen, Germany, 3–5 March 2015. [CrossRef]